

Angular dependence of the upper critical field of superconductors

W. Pitscheneder and E. Schachinger

Institut für Theoretische Physik, Technische Universität Graz, A-8010 Graz, Austria

(Received 28 July 1992)

In this paper a theory of the upper critical magnetic field, H_{c2} , of anisotropic superconductors is discussed. This theory allows the calculation of the angular dependence of H_{c2} in anisotropic systems with arbitrary impurity content. The model includes an electron-phonon-coupling anisotropy by use of a Fermi-surface-harmonics expansion. For simplicity, the model is restricted to the case of weak anisotropies. The key features of the model are discussed numerically using a simple separable model anisotropy.

I. INTRODUCTION

Anisotropy effects in superconductors have been a subject of experimental and theoretical scrutiny for almost three decades. The most pronounced effects have been reported for the upper critical field H_{c2} which, for single crystals, shows a pronounced angular dependence [as reported for instance for niobium¹ or $\text{YBa}_2\text{Cu}_3\text{O}_{7-\delta}$ (Ref. 2)]; for polycrystalline samples, on the other hand, $H_{c2}(T)$ shows a pronounced upward curvature at temperatures close to the critical one (T_c), and a low-temperature enhancement of H_{c2} in comparison to isotropic systems.^{3,4}

Theoretical progress in the description of the angular dependence of H_{c2} was primarily made in two directions. One branch followed the effective mass model (see, for instance, Kogan and Clem⁵ and references therein) which was shown by Hohenberg and Werthamer⁶ not to be applicable to cubic superconductors. The other branch pursued the approach to describe the anisotropy of the upper critical field in terms of series expansions using a suitable set of harmonic functions which reflected the basic symmetries of the lattice. (For instance, cubic harmonics were used to describe the anisotropic behavior of niobium.⁷) All these various approaches had in common that the anisotropy of H_{c2} was attributed (a) to the anisotropy of the Fermi surface which results in an anisotropic Fermi velocity, and (b) to the anisotropy in the electron-phonon-coupling process which leads to the building of the Cooper pairs. Impurity scattering and Coulomb interaction were almost generally assumed to be isotropic interactions.

The material niobium was most attractive because it showed a rather weak anisotropy of H_{c2} and it was therefore a welcomed object to test theoretical models. It was also the material where most of the progress had been achieved over the years. It started with Butler's theoretical interpretation⁸ of the niobium data of Kerchner *et al.*⁹ This analysis depended on extensive band-structure calculations and put the emphasis on the anisotropy of the Fermi velocity. The agreement with experiment was excellent. Teichler, on the other hand, developed at the

same time a semiclassical theory of H_{c2} which included Fermi surface anisotropy and electron-phonon-coupling anisotropy.¹⁰ The anisotropy of H_{c2} was expressed in terms of cubic harmonics and it proved to be quite successful in the beginning,¹¹ but later and more accurate experiments¹ showed less satisfying agreement.

The, so far, final step was made by Rieck¹² and Rieck and Scharnberg,¹³ who presented a theoretical description of the anisotropic H_{c2} for arbitrary shapes of the Fermi surface and they allowed for additional anisotropy in the electron-electron pairing term. (This opened the possibility of dropping the restriction of weak anisotropies which was genuine to all previous approaches.) Another method has recently been published by Langmann.¹⁴ His theory is in principle quite similar to the one of Rieck and Scharnberg but he treated the anisotropy of the electron-phonon-coupling process in a more concise way by using Fermi surface harmonics (FSH) as had been introduced by Allen.¹⁵

This paper expands on Langmann's approach in an attempt to shed some light on the role of the electron-phonon-coupling anisotropy in the theory of anisotropic H_{c2} . The main theoretical part is presented in Secs. II and III where we use a simple separable model anisotropy to make the mathematics more transparent. This, of course, is restricted again to weak anisotropies, which was certainly not the case in Langmann's original paper. Numerical results are then discussed in Sec. IV together with an analysis of experimental data. Finally, conclusions are drawn in Sec. V.

II. GENERAL THEORY

We introduce, according to Allen,¹⁵ a complete set of functions

$$\{\eta_{so}(\mathbf{v}_\mathbf{k}); \quad s = 1, \dots, S; \quad o = 0, \dots, \infty\} \quad (1)$$

orthonormal on the energy shell of energy E :

$$\langle \eta_{so}(\mathbf{v}_\mathbf{k}) \eta_{s'o'}(\mathbf{v}_\mathbf{k}) \rangle_E = \delta_{ss'} \delta_{oo'} \quad (2)$$

with

$$\langle f(\mathbf{k}) \rangle = \frac{1}{N(E)} \int \frac{d^3k}{(2\pi)^3} \delta(\varepsilon(\mathbf{k}) - E) f(\mathbf{k}). \quad (3)$$

Here, s is a sheet index indicating the various disjoint pieces of the energy shell, o is an order index, and $\mathbf{v}_{\mathbf{k}}$ is the particle velocity in the direction of the wave vector \mathbf{k} on the energy shell E . In particular, if $E = \varepsilon_F$, the Fermi energy, the energy shell is the Fermi surface and $\mathbf{v}_{\mathbf{k}} = \mathbf{v}_F(\mathbf{k})$, the anisotropic Fermi velocity. In this case we speak of a set of Fermi surface harmonics $\{\eta_{so}(\mathbf{v}_F(\mathbf{k}))\}$.

Any function $f(\mathbf{k})$ can be expanded

$$f(\mathbf{k}) = \sum_{s,o} \eta_{so}(\mathbf{v}_{\mathbf{k}}) f_{so}(E) \quad (4)$$

with

$$f_{so}(E) = \langle f(\mathbf{k}) \eta_{so}(\mathbf{v}_{\mathbf{k}}) \rangle_E. \quad (5)$$

The zeroth-order function is chosen to be equal to

$$\eta_{s0} = 1/\sqrt{p_s(E)}, \quad (6)$$

where we introduced the ‘‘partial’’ weight of the sth disjoint piece of the energy shell by

$$p_s(E) = N_s(E)/N(E), \quad (7)$$

where $N_s(E)$ is the partial electronic density of states

$$N_s(E) = \int_{\text{sheet } s} \frac{dS_{\mathbf{k}}}{(2\pi)^3 |\nabla \varepsilon(\mathbf{k})|}. \quad (8)$$

$N(E)$ is the the total electronic density of states. It is furthermore useful to introduce Clebsh-Gordan coefficients (CGC's)

$$C_{s_o, s'_{o'}, s''_{o''}} = C_{s, o, o' o''} = \langle \eta_{s_o}(\mathbf{v}_{\mathbf{k}}) \eta_{s'_{o'}}(\mathbf{v}_{\mathbf{k}}) \eta_{s''_{o''}}(\mathbf{v}_{\mathbf{k}}) \rangle_E, \quad (9)$$

where the first equality comes from the fact that a CGC is zero unless $s = s' = s''$. [The $\eta_{s_o}(\mathbf{v}_{\mathbf{k}})$ defined on different disjoint sheets of the energy shell are orthogonal to each other for all orders o .]

The FSH introduced here have been applied successfully by Daams,¹⁶ Daams and Carbotte,¹⁷ Allen and Mitrović,¹⁸ and in particular by Niel *et al.*¹⁹ to explain anisotropic properties in the thermodynamics of indium.

Following closely Langmann,¹⁴ a set of equations in \mathbf{k} space is found which describes in a quite general way how rather weak anisotropies influence H_{c2} . (The case of pronounced anisotropies requires more elaborate techniques.¹²⁻¹⁴) The first equation is a simple anisotropic expansion of the standard ω channel of the Eliashberg equations describing the renormalized normal-state Matsubara frequencies

$$\tilde{\omega}_n(\mathbf{k}) = \omega_n + \pi T \sum_m \int \frac{d^3k'}{(2\pi)^3} \delta(\varepsilon(\mathbf{k}') - E) V(\mathbf{k}, \mathbf{k}'; i\omega_n - i\omega_m) \text{sgn}(\omega_m), \quad (10)$$

with the anisotropic interaction potential

$$V(\mathbf{k}, \mathbf{k}'; i\omega_n - i\omega_m) = \frac{1}{N(0)} \left[\lambda(\mathbf{k}, \mathbf{k}'; i\omega_n - i\omega_m) - \Theta(\omega_c - |\omega_n|) \mu^*(\mathbf{k}, \mathbf{k}'; i\omega_c) + \frac{1}{\pi T} \delta_{mn} \gamma(\mathbf{k}, \mathbf{k}') \right], \quad (11)$$

the Matsubara frequencies $\omega_n = \pi T(2n + 1)$, $n = 0, 1, 2, \dots$, the electronic density of states at the Fermi level $N(E = \varepsilon_F = 0)$, the anisotropic electron-phonon interaction potential

$$\lambda(\mathbf{k}, \mathbf{k}'; i\omega_n - i\omega_m) = 2 \int_0^\infty d\Omega \frac{\Omega \alpha^2 F(\mathbf{k}, \mathbf{k}'; \Omega)}{\Omega^2 + (\omega_n - \omega_m)^2}, \quad (12)$$

the anisotropic electron-phonon interaction spectral function $\alpha^2 F(\mathbf{k}, \mathbf{k}'; \Omega)$, the anisotropic Coulomb interaction pseudopotential $\mu^*(\mathbf{k}, \mathbf{k}'; i\omega_c)$, which is also a function of the cutoff frequency ω_c . Finally,

$$\gamma(\mathbf{k}, \mathbf{k}') = \pi N(0) n_I |\langle \mathbf{k} | V_I | \mathbf{k}' \rangle|^2 \quad (13)$$

describes the particle scattering at randomly distributed impurity sites of concentration n_I and of the scattering potential V_I .

The second equation determines H_{c2} implicitly:

$$\phi(\mathbf{k}, i\omega_n) = -T \sum_m \int \frac{d^3k'}{(2\pi)^3} V(\mathbf{k}, \mathbf{k}'; i\omega_n - i\omega_m) \times \chi(\mathbf{k}', i\omega_m) \phi(\mathbf{k}', i\omega_m) \quad (14)$$

with

$$\chi(\mathbf{k}, i\omega_n) = \frac{1}{\alpha} \int \frac{d^2q_\perp}{(2\pi)^2} G_{H=0}(\mathbf{k} - \frac{1}{2}\mathbf{q}_\perp, i\omega_n) \times G_{H=0}^\dagger(\mathbf{k} + \frac{1}{2}\mathbf{q}_\perp, i\omega_n) \exp \left\{ -\frac{|\mathbf{q}_\perp|^2}{2\alpha} \right\} \quad (15)$$

and

$$\alpha = |e| \mu_0 H_{c2}(T). \quad (16)$$

Here, $G_{H=0}(\mathbf{k}, i\omega_n) = 1/[i\tilde{\omega}_n - \varepsilon(\mathbf{k})]$ is the normal-state Green's function for the external magnetic field $H = 0$. The integral of Eq. (15) is evaluated in a plane perpendicular to the direction of the external magnetic field (i.e., \mathbf{q}_\perp is a vector in such a plane). Equations (10), (14), and (15) reduce in the isotropic limit to the equations given by Schossmann and Schachinger for the isotropic superconductor with arbitrary impurity content.²⁰

The next step involves the expansion of all \mathbf{k} -

dependent functions in FSH according to Eq. (4). If we restrict ourselves to classical superconductors with $\varepsilon_F \gg \omega_D$, the Debye energy, then all the integrals are restricted to a small zone of width $2\omega_D$ around the

Fermi energy, and if we also assume that $N(E)$ and $V(\mathbf{k}, \mathbf{k}'; i\omega_n - i\omega_m)$ do not vary too much inside this zone, we arrive at the following set of equations for each FSH index s and o :

$$\tilde{\omega}_n(so) = \omega_n \delta_{o0} \sqrt{p_s(0)} + \pi T \sum_m \text{sgn}(\omega_m) \sum_{s'} \sqrt{p_{s'}(0)} V(so, s'o; i\omega_n - i\omega_m), \quad (17)$$

$$V(so, s'o'; i\omega_n - i\omega_m) = \lambda(so, s'o'; i\omega_n - i\omega_m) - \Theta(\omega_c - |\omega_n|) \mu^*(so, s'o'; \omega_c) + \frac{1}{\pi T} \delta_{mn} \gamma(so, s'o'), \quad (18)$$

$$\mu^*(so, s'o'; \omega_c) = \mu^*(so, s'o'; E, E', \omega_c)|_{E=E'=\text{const}}, \quad (19)$$

$$\phi_{so}(i\omega_n) = \pi T \sum_{\omega_m \leq \omega_c} \sum_{s'o'o''} C_{s'o'o''} V(so, s'o'; i\omega_n - \omega_m) \chi_{s'o''}(i\omega_m) \phi_{s'o''}(i\omega_m), \quad (20)$$

$$\chi_{so}(i\omega_n) = \left\langle \frac{1}{\tilde{\omega}_n(\mathbf{k})} \sqrt{\pi} x \exp(x^2) \text{erfc}(x) \eta_{so}(\mathbf{v}_\mathbf{k}) \right\rangle_{\varepsilon_F}, \quad (21)$$

and

$$x = \frac{|\tilde{\omega}_n(\mathbf{k})|}{|\mathbf{v}_\perp(\mathbf{k})| \sqrt{\alpha/2}}, \quad \alpha = |e| \mu_0 H_{c2}(T). \quad (22)$$

As $\mathbf{v}_\perp(\mathbf{k})$ is the particle velocity in the plane perpendicular to the external magnetic field, it is obvious that the set of equations (17)–(22) describes the upper critical field of an anisotropic superconductor as a function of its orientation with respect to the direction of the external field. An additional angular dependence of H_{c2} is provided implicitly by the $\tilde{\omega}_n(so)$ because of the anisotropic coupling potential.

In passing we would like to point out that in the limit $H_{c2} \rightarrow 0$ Eqs. (17)–(22) reduce to the anisotropic T_c equations given by Allen and Mitrović.¹⁸ Equation (21) was reported in similar form by Rieck,¹² Hohenberg and Werthamer,⁶ and Youngner and Klemm.²¹

III. APPLICATION TO A SEPARABLE MODEL ANISOTROPY

A separable model anisotropy was introduced by Markovitz and Kadanoff²² for the effective electron-electron-coupling potential of the BCS theory. It is, in our case, of the form

$$\lambda(\mathbf{k}, \mathbf{k}'; i\omega_n - i\omega_m) = \lambda(i\omega_n - i\omega_m) [1 + a(\mathbf{k})] [1 + a(\mathbf{k}')], \quad (23)$$

where the anisotropy function $a(\mathbf{k})$ has the property

$$\langle a(\mathbf{k}) \rangle_{\varepsilon_F} = 0, \quad (24)$$

and only terms of the order $\langle a(\mathbf{k})^2 \rangle_{\varepsilon_F} = \langle a^2 \rangle$ are kept. Finally, $\lambda(i\omega_n - i\omega_m)$ is given by

$$\lambda(i\omega_n - i\omega_m) = 2 \int_0^\infty d\Omega \frac{\Omega \alpha^2 F(\Omega)}{\Omega^2 + (\omega_n - \omega_m)^2}, \quad (25)$$

with $\alpha^2 F(\Omega)$ the electron-phonon interaction spectral

function of the isotropic system. A similar ansatz was used by Teichler²³ for the Fermi velocity, but we follow the notation used by Prohammer and Schachinger²⁴ and define the anisotropic Fermi velocity as

$$|\mathbf{v}(\mathbf{k})| = \langle |\mathbf{v}_F| \rangle_{\varepsilon_F} [1 + b(\mathbf{k})], \quad (26)$$

with the anisotropy function $b(\mathbf{k})$ having the same properties as $a(\mathbf{k})$.

The simplest model is found by dividing the spherical Fermi surface into two parts on which $a(\mathbf{k})$ and $b(\mathbf{k})$ take on appropriate constant values (Fig. 1). This restricts the FSH series expansions to zeroth-order terms on each sheet, resulting in an effective two-band model. If we choose values for $\langle a^2 \rangle$ and $\langle b^2 \rangle$ it is quite easy to calculate the functions $a(\mathbf{k})$ and $b(\mathbf{k})$. We find ($p_1 = p_1(0)$, $p_2 = p_2(0)$):

$$a(\mathbf{k}) = \begin{cases} a_1^\pm = \pm \sqrt{\langle a^2 \rangle p_2 / p_1}, & \text{sheet 1} \\ a_2^\pm = \mp \sqrt{\langle a^2 \rangle p_1 / p_2}, & \text{sheet 2} \end{cases} \quad (27)$$

and

$$b(\mathbf{k}) = \begin{cases} b_1 = \sqrt{\langle b^2 \rangle p_2 / p_1}, & \text{sheet 1} \\ b_2 = -\sqrt{\langle b^2 \rangle p_1 / p_2}, & \text{sheet 2.} \end{cases} \quad (28)$$

This results in the Fermi velocities

$$v_F(\mathbf{k}) = \begin{cases} v_{F1} = \langle |\mathbf{v}_F| \rangle_{\varepsilon_F} \left(1 + \sqrt{\langle b^2 \rangle p_2 / p_1} \right), & \text{sheet 1} \\ v_{F2} = \langle |\mathbf{v}_F| \rangle_{\varepsilon_F} \left(1 - \sqrt{\langle b^2 \rangle p_1 / p_2} \right), & \text{sheet 2} \end{cases} \quad (29)$$

for the two sheets. The \pm symbol in Eq. (27) reflects the remaining ambiguity whether the electron-phonon-coupling anisotropy is in phase with the Fermi velocity anisotropy (plus sign on the Fermi surface sheet 1) or not (minus sign). The zeroth-order FSH follows from Eq. (6):

$$\eta_{1,2} = 1/\sqrt{p_{1,2}}. \quad (30)$$

The $\lambda(so, s'o'; i\omega_n - i\omega_m)$ of Eq. (18) simplifies to

$$\begin{aligned}
\lambda(s_0, s'_0; i\omega_n - i\omega_m) &= \lambda(s_0, s'_0; i\omega_n - i\omega_m) \\
&= \langle \langle \lambda(i\omega_n - i\omega_m) [1 + a(\mathbf{k})] [1 + a(\mathbf{k}')] \eta_{s_0}(\mathbf{v}_\mathbf{k}) \eta_{s'_0}(\mathbf{v}_{\mathbf{k}'}) \rangle_{\varepsilon_F} \rangle_{\varepsilon_F} \\
&= \lambda(i\omega_n - i\omega_m) \sqrt{p_s p_{s'}} (1 + a_s) (1 + a_{s'}).
\end{aligned} \tag{31}$$

The Coulomb interaction pseudopotential simplifies to

$$\mu^*(s_0, s'_0; \omega_c) = \sqrt{p_s p_{s'}} \mu^*(\omega_c) \tag{32}$$

and the impurity interaction is now described by

$$\gamma(s_0, s'_0) = \sqrt{p_s p_{s'}} \gamma. \tag{33}$$

Collecting all the results, we find for the renormalized Matsubara frequencies the equation

$$\begin{aligned}
\tilde{\omega}_n(s) &= \sqrt{p_s} \left\{ \omega_n + \pi T \sum_m \text{sgn}(\omega_m) \lambda(i\omega_n - i\omega_m) \right. \\
&\quad \left. \times (1 + a_s) + \gamma \text{sgn}(\omega_n) \right\},
\end{aligned} \tag{34}$$

which still reflects the anisotropy of the electron-phonon-coupling process in anisotropic, sheet-dependent, renormalized Matsubara frequencies. The upper critical field is determined from

$$\begin{aligned}
\phi_s(i\omega_n) &= \pi T \sqrt{p_s} \sum_{\omega_m \leq \omega_c} \sum_{s'} V(s, s'; i\omega_n - i\omega_m) \\
&\quad \times \chi_{s'}(i\omega_m) \phi_{s'}(i\omega_m)
\end{aligned} \tag{35}$$

with

$$\chi_s(i\omega_n) = \left\langle \frac{1}{|\tilde{\omega}_n(s)|} \sqrt{\pi} x \exp(x^2) \text{erfc}(x) \xi_s \right\rangle_{\varepsilon_F} \tag{36}$$

and

$$\xi_s = \begin{cases} 1, & \text{on sheet } s \\ 0, & \text{outside sheet } s \end{cases} \tag{37}$$

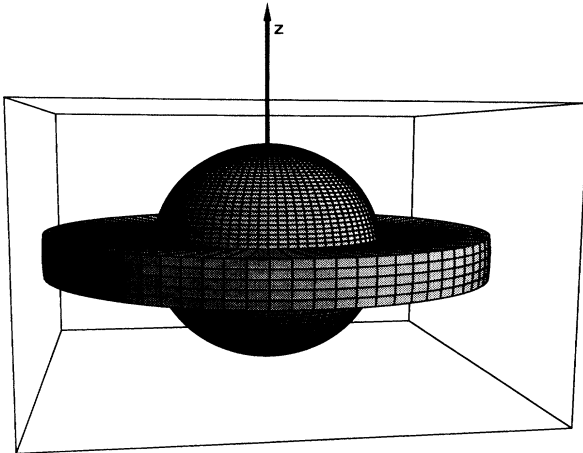


FIG. 1. The simplest Fermi surface model describing a separable model anisotropy ($\langle b^2 \rangle = 0.118$).

$$\begin{aligned}
V(s, s'; i\omega_n - i\omega_m) &= \lambda(i\omega_n - i\omega_m) (1 + a_s) (1 + a_{s'}) \\
&\quad - \Theta(\omega_c - |\omega_n|) \mu^*(\omega_c) + \delta_{mn} t^+,
\end{aligned} \tag{38}$$

$$t^+ = \frac{\gamma}{\pi T}. \tag{39}$$

If we multiply Eqs. (34), (35), and (36) on both sides by $1/\sqrt{p_s}$ and rename $\tilde{\omega}_n(s)/\sqrt{p_s}$ by $\tilde{\omega}_n(s)$, etc., those equations become almost identical to equations given by Prohammer and Schachinger for the weakly anisotropic polycrystalline superconductor.²⁴ The only difference exists in Eq. (36), which depends explicitly on the orientation of the external magnetic field with respect to the symmetry axis of the Fermi surface (in our model of Fig. 1, the z axis).

This striking similarity is suggestive enough to define a polycrystalline limit of the above equations. The polycrystal is assumed to consist of a large number of small, randomly oriented crystallites. It should then be possible to perform a transition from Eqs. (34)–(36) to the results of Prohammer and Schachinger by calculating the polycrystalline average of Eq. (36):

$$\chi_{\text{poly},s}(i\omega_n) = \langle \chi_{\text{single},s}(i\omega_n) \rangle_{\text{poly}}. \tag{40}$$

Here, $\langle \dots \rangle_{\text{poly}}$ denotes the directional average over the space angle Ω which parametrizes each particular $\chi_{\text{single},s}(i\omega_n)$ and which describes the orientation of this particular crystallite with respect to the external magnetic field.

It is almost impossible to perform the average in Eq. (40) analytically and, therefore, we would like to follow a more argumentative path: we reflect on the fact that $\chi_{\text{single},s}(i\omega_n)$ is itself determined from a Fermi surface average and, thus, Eq. (40) contains two subsequent averaging procedures. Such a procedure can be understood as an analog to two subsequent mappings which can be substituted by one composite mapping. We write explicitly

$$\langle \chi_{\text{single},s}(i\omega_n) \rangle_{\text{poly}} = \langle \langle \dots \xi_s \rangle_{\varepsilon_F, \text{single}} \rangle_{\text{poly}} \tag{41}$$

and recognize that we actually perform an orientational average over the Fermi surfaces of the various crystallites. This results in an “effective Fermi surface” having only the weight p_s because of the factor ξ_s in Eq. (41).

Since we use a separable model to describe the anisotropies, this effective Fermi surface will be a sphere and the system consists now of S spheres of weight p_s :

$$\chi_{\text{poly},s}(i\omega_n) = p_s \langle \dots \rangle_{\text{sphere},s}. \tag{42}$$

This process is applied on Eq. (36) and it results in

$$\begin{aligned}
\chi_{\text{poly},s}(i\omega_n) &= \left\langle \frac{1}{|\tilde{\omega}_s(n)|} \sqrt{\pi} x \exp(x^2) \text{erfc}(x) \right\rangle_{\text{sphere}} \\
&= \frac{2}{\sqrt{\beta_s}} \int_0^\infty d\zeta \exp(-\zeta^2) \tan^{-1} \left(\frac{\sqrt{\beta_s}}{\tilde{\omega}_s(n)} \zeta \right),
\end{aligned} \tag{43}$$

with

$$\beta_s = \frac{1}{2}|e|\mu_0 H_{c2} [\langle |\mathbf{v}_F| \rangle_{\varepsilon_F} (1 + b_s)]^2. \quad (44)$$

Equation (43) does not contain any directional dependence and corresponds to the expression used in Ref. 24. [The authors of that paper used an *ad hoc* ansatz to arrive at expression (43).]

IV. NUMERICAL RESULTS

A. The influence of the electron-phonon coupling anisotropy

The similarity of our Eqs. (34)–(36) to the ones used by Prohammer and Schachinger²⁴ allows the applications of techniques described by those authors in detail to simplify numerics significantly. We use in all our calculations the $\alpha^2 F(\Omega)$ of niobium measured by Arnold *et al.*,²⁵ the anisotropy parameters $\langle a^2 \rangle = 0.0335$ and $\langle b^2 \rangle = 0.118$, and a Fermi velocity of $v_F = 0.57 \times 10^6 \text{ ms}^{-1}$.³ The anisotropy of the Fermi velocity is out of phase with the electron-phonon coupling anisotropy according to Crabtree *et al.*,²⁶ and the Fermi surface model is that of Fig. 1 with equal weights $p_1 = p_2 = 0.5$ for both sheets.

We should note in passing that our weak anisotropy approach is only correct as long as the external magnetic field is parallel to the z axis. The approximation becomes worse the more the external magnetic-field orientation deviates from this direction. Rieck¹² reported that a *full* theory results in significant deviations from the weak anisotropy approximation in such cases. But,

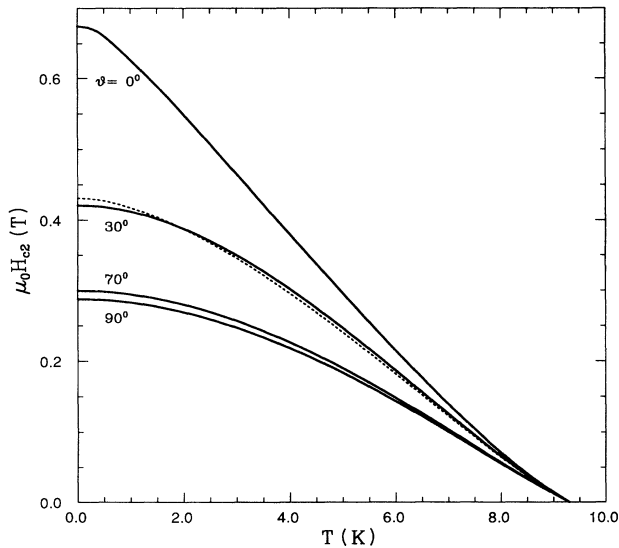


FIG. 2. The temperature dependence of the upper critical field $H_{c2}(T)$ for different orientations ϑ of the external magnetic field \mathbf{H} with respect to the horizontal plane of the Fermi surface represented in Fig. 1. Clean limit model: $t^+ = 0$ meV; the other parameters are $\langle a^2 \rangle = 0.0335$, $\langle b^2 \rangle = 0.118$, and $v_F = 0.57 \times 10^6 \text{ ms}^{-1}$. The dashed line corresponds to the $H_{c2}(T)$ of a polycrystalline sample having the same anisotropy parameters and the same Fermi velocity.

as we only want to study qualitative effects, we believe that the use of our grossly simplified theory is justified.

Figure 2 shows the temperature dependence $H_{c2}(T)$ for various orientations ϑ of the external magnetic field ($\vartheta = 0$, \mathbf{H} is in the horizontal plane) in the clean limit, $t^+ = 0$ meV. We see a very pronounced — unrealistic — angular dependence of $H_{c2}(T)$ and it is most remarkable that all the $H_{c2}(T, \vartheta)$ curves show a pronounced upward curvature in the temperature region close to T_c . (Such an upward curvature was observed on niobium single crystals;¹ see also Fig. 12 of Ref. 3.)

Our model allows us to “switch off” either anisotropy in setting the respective anisotropy parameter equal to zero. Setting $\langle b^2 \rangle = 0$ (no Fermi velocity anisotropy) results in a still anisotropic $H_{c2}(T, \vartheta)$ as is shown in Fig. 3. This results from the fact that $\chi_s(i\omega_n)$ is still anisotropic because of the explicit $\tilde{\omega}_s(n)$ anisotropy. (Nevertheless, each change in $\langle b^2 \rangle$ results in a change of the geometry of the separable model anisotropy in order to keep $p_1 = p_2 = 0.5$. Our numerical results indicated that these influences are of minor importance and we therefore refrain from an exhaustive discussion of this point.)

The most interesting feature is found by comparing the curvature of $H_{c2}(T, \vartheta)$ close to T_c in both models. This is done in Fig. 4. We see that the model with $\langle b^2 \rangle \neq 0$ shows an upward curvature in that region while the model with $\langle b^2 \rangle = 0$ shows the accustomed downward curvature. (This justifies in retrospect the fitting procedure employed by Weber *et al.*,³ who fitted $\langle b^2 \rangle$ and v_F to the high-temperature data.)

Figure 5, finally, shows the angular dependence of H_{c2} for various fixed temperatures. We see that the angular dependence is most pronounced at $T = 0$ and becomes almost indistinguishable for $T \sim T_c$. It is interesting to note that Welp *et al.*² report a similar angular dependence for the high-temperature superconduc-

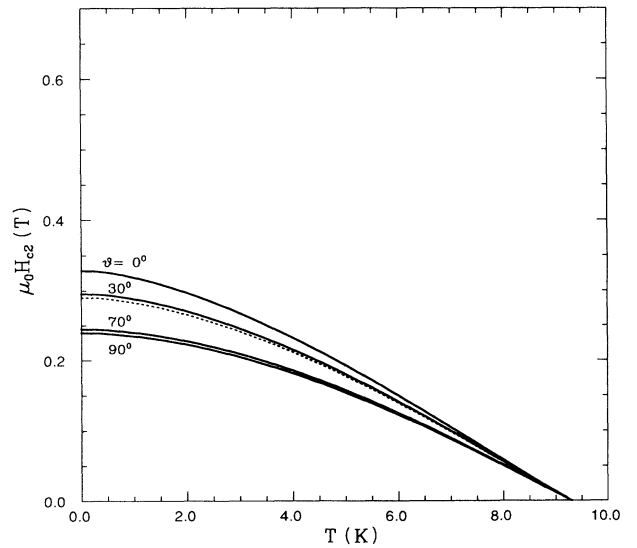


FIG. 3. The same as Fig. 2 with $\langle b^2 \rangle = 0$.

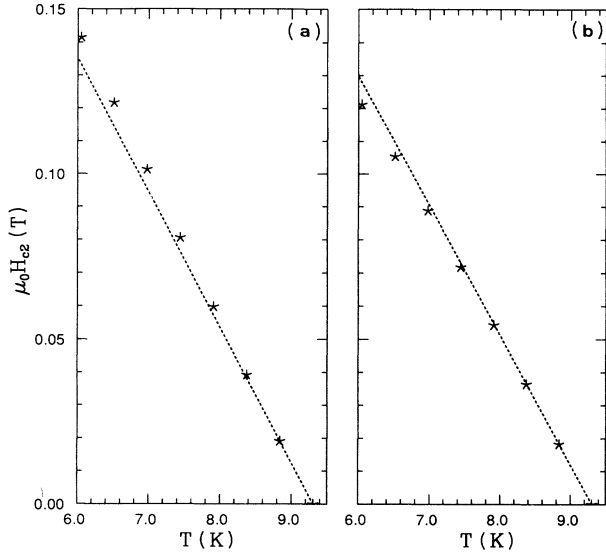


FIG. 4. The curvature of $H_{c2}(T)$ for $\varphi = 90^\circ$. (a) $\langle b^2 \rangle = 0.118$ and (b) $\langle b^2 \rangle = 0$. The dashed line indicates the slope of $H_{c2}(T)$ at T_c while the \star symbols indicate the numerical results.

tor $\text{YBa}_2\text{Cu}_3\text{O}_{7-\delta}$. They used an effective mass model for a fit to their data and indeed, our model Fermi surface of Fig. 1 could be regarded as a separable model approach to an ellipsoidal Fermi surface. (A similar angular distribution of H_{c2} is found for cylinder symmetrical Fermi surfaces, which are more likely for high-temperature superconductors.²⁷) On the other hand, a comparison with the experimental data of Sauerzopf *et al.*¹ proves immediately that we do not get the proper angular dependence. Niobium shows an absolute min-

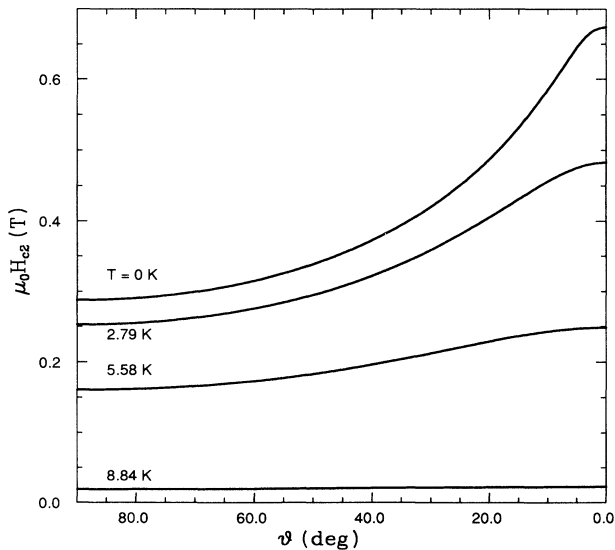


FIG. 5. The angular dependence of $H_{c2}(T, \varphi)$ for various temperatures $T < T_c$.

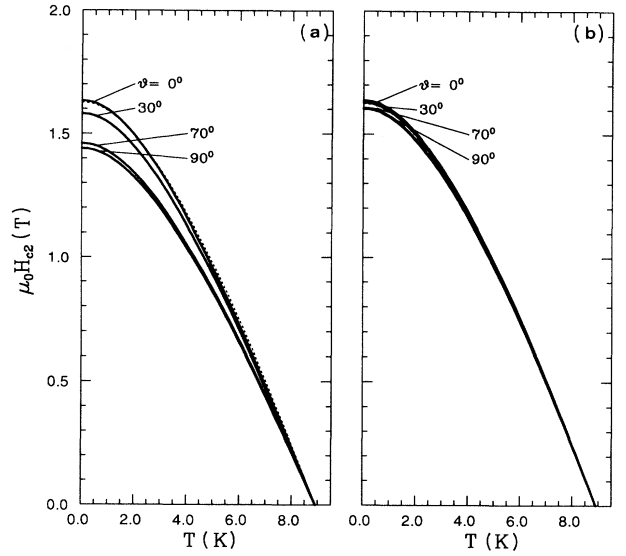


FIG. 6. Same as Fig. 2 but in the almost dirty limit, $t^+ = 10$ meV. (a) $\langle b^2 \rangle = 0.118$ and (b) $\langle b^2 \rangle = 0$.

imum for the [100] direction, a local minimum for the [110] direction, and a maximum for the [111] direction. If we assume the z axis to be parallel to the [100] direction, the maximum should then appear at an angle of $\varphi = 35.26^\circ$, which is obviously not the case in our model calculation. Section IV B elaborates on this point.

We can also study the influence of the electron-phonon-coupling anisotropy by adding impurities to the system which will result in a “washing out” of this anisotropy.²² Figure 6 studies the situation close to the dirty limit, $t^+ = 10$ meV. It compares the two systems with [Fig. 6(a)] and without [Fig. 6(b)] Fermi velocity anisotropy. We see that the system with $\langle b^2 \rangle = 0$ has an almost negligible anisotropy of H_{c2} even close to $T = 0$, while the other system still shows a quite pronounced anisotropy of H_{c2} .

These results suggest a possibility to assess the amount of electron-phonon-coupling anisotropy by experiment: in starting with a high-purity single crystal we measure the angular dependence of H_{c2} at some low temperature $T \ll T_c$ and successively increase the impurity content. In doing so, we smear out the electron-phonon-coupling anisotropy and a theoretical analysis of the experimental data will then allow us to derive the desired information about the coupling anisotropy directly.

B. A separable model anisotropy of cubic symmetry

The model Fermi surface of Fig. 1 did not have cubic symmetry and was, therefore, insufficient to reproduce the angular dependence of H_{c2} as observed for niobium. Figure 7 presents a Fermi surface which is of cubic symmetry; it also allows us to formulate a separable model anisotropy according to Sec. III. The model represented in Fig. 7 has a Fermi velocity anisotropy of $\langle b^2 \rangle = 0.1$ which is a bit smaller than the value of 0.118 suggested

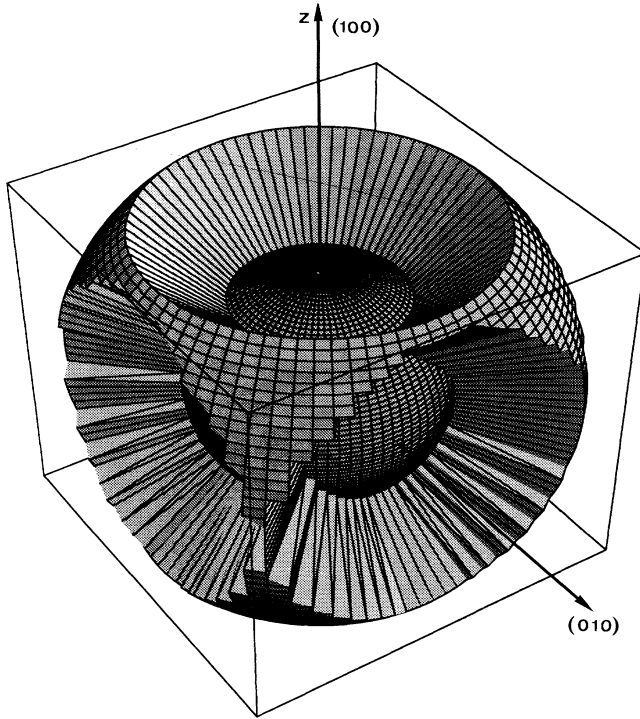


FIG. 7. A Fermi surface of cubic symmetry. It corresponds to an anisotropy parameter of $\langle b^2 \rangle = 0.1$.

by the analysis of polycrystalline H_{c2} data. This value could not be realized because of geometrical reasons. The weight of both sheets is, again, 0.5.

We calculate the angular dependence of H_{c2} for a tem-

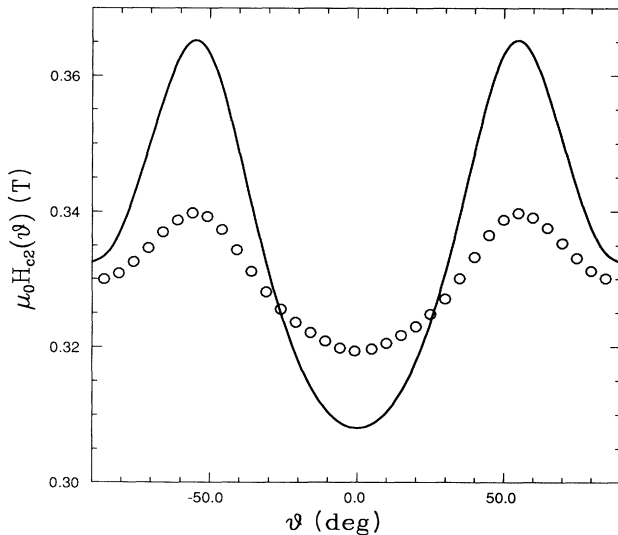


FIG. 8. The angular dependence of $H_{c2}(T)$ for $T = 3$ K and the Fermi surface model of Fig. 7. $\langle a^2 \rangle = 0.0335$ and $v_F = 0.57 \times 10^6$ ms^{-1} , and $t^+ = 0$ meV. The open circles correspond to experimental data of a high-purity niobium single crystal at the same temperature (Ref. 1).

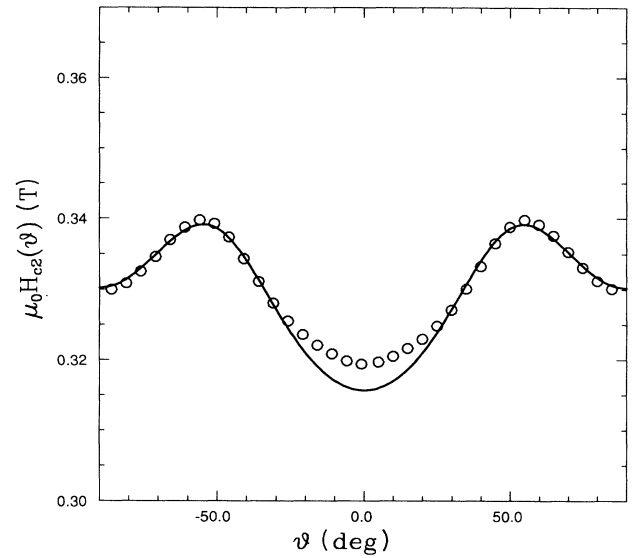


FIG. 9. The same as Fig. 8 but now for $\langle a^2 \rangle = 0.01$ and $\langle b^2 \rangle = 0.02$.

perature of 3 K in the clean limit keeping $\langle a^2 \rangle = 0.0335$ and $v_F = 0.57 \times 10^6$ ms^{-1} . Figure 8 compares our results with the experimental data of Ref. 1. We see that our model reproduces perfectly the angular dependence of H_{c2} having all the minima and maxima at the proper places. Nevertheless, the anisotropy of H_{c2} is still too large. Reducing $\langle a^2 \rangle$ to 0.01 and $\langle b^2 \rangle$ to 0.02 results, finally, in an almost perfect match between theory and experiment (Fig. 9).

This result certainly does not render the analysis of Weber *et al.*³ obsolete. First of all, our cubic-symmetry Fermi surface is obviously not a good model of the real Fermi surface of niobium which consists of three disjoint pieces²⁸ while our model consists of only two. Furthermore, the external magnetic field “sees” in most cases two of the disjoint pieces of the real Fermi surface, which results in some average “effective Fermi velocity” that we will have to set in correspondence to the Fermi velocity of the one single sheet that is seen by the external field in our cubic-symmetry model. Moreover, the cubic-symmetry model always has $\mathbf{v}_F \parallel \mathbf{k}$, which certainly is not the case in the real metal. This will, necessarily, make the anisotropy parameters of the simple model of Fig. 8 smaller if one wants to reproduce the observed angular dependence of H_{c2} quantitatively. Thus, the anisotropy parameters of our cubic-symmetry Fermi surface necessary to reproduce quantitatively the observed angular dependence of H_{c2} in niobium are in no correspondence to the real anisotropy of the Fermi velocity and of the electron-phonon coupling.

V. CONCLUSION

We discussed a theory of H_{c2} for weakly anisotropic superconductors which allows the calculation of the angular and temperature dependence of H_{c2} for arbitrary

impurity contents. Our main results are the following:

(i) The electron-phonon-coupling anisotropy gives a significant contribution to the overall anisotropy of H_{c2} . It cannot be disregarded as was done so often in the past. Increasing the impurity content of a single crystal tends to wash out this anisotropy and this property allows us to set up an experimental program for a closer investigation of the influence of the electron-phonon-coupling anisotropy.

(ii) The upward curvature of $H_{c2}(T)$ close to T_c is a result of the Fermi velocity anisotropy. It vanishes if this anisotropy is "shut off."

(iii) The angular dependence of H_{c2} reflects the gross symmetries of the single-crystal lattice. It cannot be used as a direct Fermi surface probe like the de Haas-van Alphen effect. This is a result of the remaining Fermi surface average of Eq. (36).

(iv) Using a separable model anisotropy allows us in principle to reproduce the angular dependence of H_{c2} as long as the model reflects the gross symmetries of the crystal lattice. The anisotropy parameters found from such a comparison are not necessarily representative for

the situation in the real material. A realistic theoretical analysis of the angular dependence of H_{c2} would certainly require a more realistic Fermi surface model, i.e., the use of three disjoint Fermi surface sheets in the case of niobium and an expansion to higher-order FSH on each sheet as it was discussed by Butler and Allen,²⁹ and a directional-dependent $\alpha^2 F(\Omega)$.³⁰

(v) The *ad hoc* model of Prohammer and Schachinger²⁴ for the upper critical field in anisotropic polycrystals is valid in the limit of weak anisotropies. This explains the excellent agreement between this theory and experiments reported for polycrystalline niobium.³

ACKNOWLEDGMENTS

The authors are grateful to Dr. E. Langmann for many suggestions and inspired discussions. We are also grateful to Dr. F. Sauerzopf for providing us with the original experimental data of the high-purity niobium single crystal. We would also like to thank Professor K. Scharnberg for his interest in this work.

¹F.M. Sauerzopf, E. Moser, H.W. Weber, and F.A. Schmidt, *J. Low Temp. Phys.* **66**, 191 (1987).

²U. Welp, M. Grimsditch, H. You, W.K. Kwok, M.M. Fang, G.W. Crabtree, and J.Z. Liu, *Physica C* **161**, 1 (1989).

³H.W. Weber, E. Seidl, C. Laa, E. Schachinger, M. Prohammer, A. Junod, and D. Eckert, *Phys. Rev. B* **44**, 7585 (1991).

⁴E. Schachinger and M. Prohammer, *Physica C* **156**, 701 (1988).

⁵V.G. Kogan and J.R. Clem, *Phys. Rev. B* **24**, 2497 (1981).

⁶P.C. Hohenberg and N.R. Werthamer, *Phys. Rev.* **153**, 493 (1966).

⁷K. Takanaka and T. Nagashima, *Prog. Theor. Phys.* **43**, 18 (1970).

⁸W.H. Butler, *Phys. Rev. Lett.* **44**, 1516 (1980).

⁹H.R. Kerchner, D.K. Christen, and S.T. Sekula, *Phys. Rev. B* **21**, 86 (1980).

¹⁰H. Teichler, in *Anisotropy Effects in Superconductors*, edited by H.W. Weber (Plenum, New York, 1977), p. 75.

¹¹E. Seidl, H.W. Weber, and H. Teichler, *J. Low Temp. Phys.* **37**, 639 (1979).

¹²C.T. Rieck, Ph.D. thesis, University of Hamburg, 1991 (unpublished).

¹³C.T. Rieck and K. Scharnberg, *Physica B* **163**, 670 (1990).

¹⁴E. Langmann, *Phys. Rev. B* **46**, 9104 (1992).

¹⁵P.B. Allen, *Phys. Rev. B* **13**, 1416 (1976).

¹⁶J.M. Daams, Ph.D. thesis, McMaster University, 1977 (unpublished).

¹⁷J.M. Daams and J.P. Carbotte, *J. Low Temp. Phys.* **43**, 263 (1981).

¹⁸P.B. Allen and B. Mitrović, in *Solid State Physics*, Vol. **37**, edited by F. Seitz, D. Turnbull, and H. Ehrenreich (Academic, New York, 1982).

¹⁹L. Niel, N. Giesinger, H.W. Weber, and E. Schachinger, *Phys. Rev. B* **32**, 2976 (1985).

²⁰M. Schossmann and E. Schachinger, *Phys. Rev. B* **33**, 6123 (1986).

²¹D.W. Youngner and R.A. Klemm, *Phys. Rev. B* **21**, 3890 (1980).

²²D. Markovitz and L.P. Kadanoff, *Phys. Rev.* **131**, 563 (1963).

²³H. Teichler, *Phys. Status Solidi B* **69**, 501 (1975).

²⁴M. Prohammer and E. Schachinger, *Phys. Rev. B* **36**, 8353 (1987).

²⁵G.B. Arnold, J. Zasadzinski, J.W. Osnum, and E.L. Wolf, *J. Low Temp. Phys.* **40**, 225 (1980).

²⁶G.W. Crabtree, D.H. Dye, D.P. Karim, S.A. Campbell, and J.B. Ketterson, *Phys. Rev. B* **35**, 1728 (1987).

²⁷W. Pint, *Physica C* **168**, 143 (1990).

²⁸L.F. Matheiss, *Phys. Rev. B* **1**, 373 (1970).

²⁹W.H. Butler and P.B. Allen, in *Superconductivity in d- and f-Band Metals*, edited by D.H. Douglass (Plenum, New York, 1976).

³⁰E.L. Wolf, T.P. Chen, and D.M. Burnell, *Phys. Rev. B* **31**, 6069 (1985).

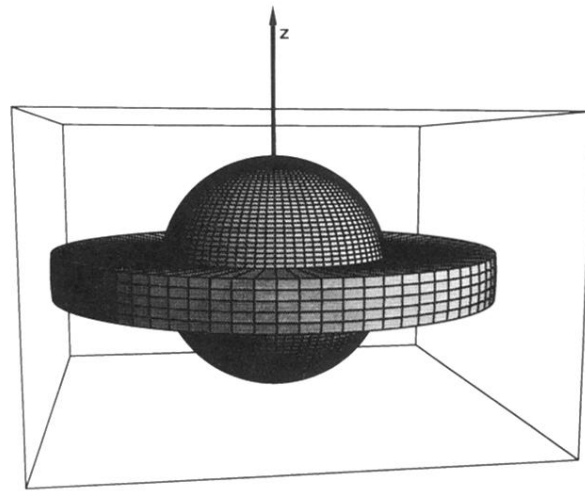


FIG. 1. The simplest Fermi surface model describing a separable model anisotropy ($\langle b^2 \rangle = 0.118$).

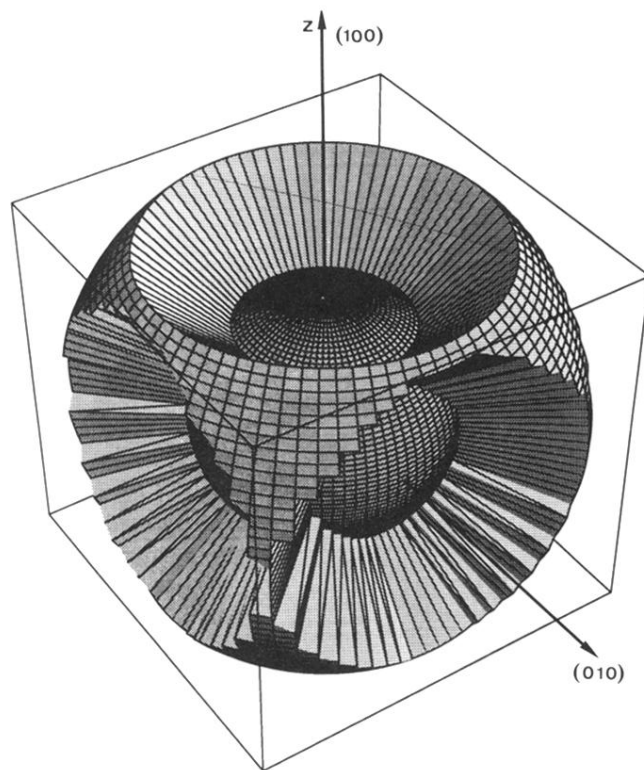


FIG. 7. A Fermi surface of cubic symmetry. It corresponds to an anisotropy parameter of $\langle b^2 \rangle = 0.1$.